Non-Brownian diffusion and chaotic rheology of autophoretic disks

R. Kailasham and Aditya S. Khair[*]

Department of Chemical Engineering, Carnegie Mellon University, Pittsburgh, Pennsylvania 15213, USA

The dynamics of a two-dimensional autophoretic disk is quantified as a minimal model for the chaotic trajectories undertaken by active droplets. Via direct numerical simulations, we show that the mean-square displacement of the disk in a quiescent fluid is linear at long times. Surprisingly, however, this apparently diffusive behavior is non-Brownian, owing to strong cross correlations in the displacement tensor. The effect of a shear flow field on the chaotic motion of an autophoretic disk is examined. Here, the stresslet on the disk is chaotic for weak shear flows; a dilute suspension of such disks would exhibit a chaotic shear rheology. This chaotic rheology is quenched first into a periodic state and ultimately a steady state as the flow strength is increased.

I. INTRODUCTION

An oil (or water) droplet immersed in a surfactant solution above the critical micelle concentration isotropically emits swollen micelles from its surface. The diffusiophoretic interaction between the droplet and its products of solubilization could result in spontaneous self-propulsion of the droplet, through a symmetry-breaking instability [1–6]. This instability occurs when the Péclet number (Pe), i.e., the dimensionless ratio of the strength of advective to diffusive transport of the products of solubilization, exceeds a critical value. Such active droplets display varying patterns of motion, including straight, curvilinear, or meandering, as Pe is increased, before entering a chaotic regime at high enough values of the Péclet number [7,8]. The occurrence of chaotic dynamics [9,10] is intriguing since the fluid flow around the drop is at low Reynolds number, where nonlinear inertial forces are absent.

In this article, we consider a two-dimensional autophoretic disk as a minimal model for an active drop (see the Supplemental Material [11] for the rationale behind this representation) and discover two important features about its dynamics. First, although such particles undergo normal diffusion at long time scales [12], we show that they are not Brownian due to strong cross correlations in their displacement components. Second, we calculate the motion of an autophoretic disk in a shear flow field. Here, the velocity and stresslet of the disk are chaotic at low values of the shear rate, implying that a dilute suspension of disks would exhibit a chaotic shear rheology. On increasing the strength of the shear flow (at fixed Péclet number) the chaos is quenched, such that the rheology becomes periodic and eventually steady. Thus we illustrate that external flows have a dramatic influence on the dynamics of autophoretic disks and, more generally, active droplets.

II. MODEL AND GOVERNING EQUATIONS

Our model consists of a circular disk of radius a^* that is immersed in an incompressible Newtonian solvent of viscosity η^* at temperature T^*. A steady simple shear flow with shear rate $\dot{\gamma}^*$ is imposed on the fluid, whose flow obeys the Stokes equations. The disk isotropically emits solute particles from its surface at a rate $\mathcal{A}^*$ and the solute diffusivity is D^*. The uniform solute concentration far away from the disk is C_∞^* and the excess solute concentration with respect to this far-field value is denoted by $c^* = C^* - C_\infty^*$. The disk interacts with the solute particles through a short-ranged potential of characteristic length b^*, which is much smaller than the radius of the disk [13]. These interactions set up a tangential phoretic slip velocity, whose magnitude is determined by a mobility parameter $\mathcal{M}^* = \pm k_B T^* b^{*2}/\eta^*$, where k_B is Boltzmann's constant, and the concentration gradient on the surface of the disk. The sign of the mobility parameter is positive (negative) for repulsive (attractive) interactions [14]. Following [15–17], the scales for length, time, fluid velocity, pressure, and concentration are defined as a^*, $a^* D^*/|\mathcal{A}^* \mathcal{M}^*|$, $U^* = |\mathcal{A}^* \mathcal{M}^*|/D^*$, $\eta^* U^*/a^*$, and $a^* |\mathcal{A}^*|/D^*$, respectively. It is convenient to define the scaled emission rate and mobility parameter as $A = \mathcal{A}^*/|\mathcal{A}^*|$ and $M = \mathcal{M}^*/|\mathcal{M}^*|$, respectively. The onset of phoretic self-propulsion requires $AM > 0$ [16,18] and we set $A = M = 1$ henceforth. The intrinsic Péclet number quantifies the chemical activity of the disk and is defined as $\mathrm{Pe} = a^* |\mathcal{A}^* \mathcal{M}^*|/D^{*2}$. The dimensionless shear rate is given by $\epsilon = \dot{\gamma}^* a^* D^*/|\mathcal{A}^* \mathcal{M}^*|$, which can be viewed as a ratio of phoretic to flow time scales.

The fluid flow and solute concentration fields around the autophoretic disk placed in an ambient shear flow are calculated by simultaneously solving the transient advection-diffusion equation for the solute concentration and the quasisteady Stokes equations

$$\mathrm{Pe}\left(\frac{\partial c}{\partial t} + \boldsymbol{v} \cdot \boldsymbol{\nabla} c\right) = \nabla^2 c, \quad \boldsymbol{\nabla} p = \nabla^2 \boldsymbol{v}, \quad \boldsymbol{\nabla} \cdot \boldsymbol{v} = 0, \quad (1)$$

———
*akhair@andrew.cmu.edu

with t, $\boldsymbol{v}$, and p denoting the dimensionless time, velocity, and pressure, respectively, and subject to $(\partial c/\partial r)(1, \theta, t) = -A$, and the attenuation condition $c(r \to \infty, t) \to 0$. The neglect of the time derivative of the velocity field in (1) is justified provided that the ratio of the kinematic viscosity of the fluid to the solute diffusivity is large [11], which is typically true for active droplet systems [1,3,8,19]. In numerical computations we employ a finite size of the computational domain, R_o, and impose the far-field Dirichlet condition $c(r = R_o) = 0$. Considering a frame of reference attached to the centroid of the disk, the slip velocity at the surface of the disk is given by $\boldsymbol{v}(r = 1, \theta) = \boldsymbol{v}_s = M\nabla_s c$, with the surface-gradient operator defined as $\nabla_s = (1/r)\boldsymbol{e}_\theta \partial/\partial\theta$, where $\boldsymbol{e}_\theta$ is the unit vector in the tangential direction, θ. The far-field velocity is given by $\boldsymbol{v}(R_o, \theta) = -\boldsymbol{U} + \epsilon y \boldsymbol{e}_x$, where $\boldsymbol{e}_x$ is the Cartesian unit vector in the x direction, y is the coordinate in the direction of the shear gradient, and the phoretic velocity $\boldsymbol{U}(t)$ may be evaluated from the slip velocity using the reciprocal theorem [20,21] as

$$\boldsymbol{U}(t) = -\frac{1}{2\pi}\int_0^{2\pi} \boldsymbol{v}_s d\theta. \tag{2}$$

The external shear acts to distort the solute field by contributing to the velocity field $\boldsymbol{v}$, which subsequently also affects the phoretic velocity $\boldsymbol{U}(t)$. The time-dependent base state, $c_0(r, \theta, t)$, corresponding to the state of zero phoretic motion [$\boldsymbol{U}(t) = 0$] is computed by solving the transient advection-diffusion equation subject to an initial condition of $c_0(r, \theta, t = 0) = 0$ over a duration t_b, at specified Pe and ϵ. The value of the base state at t_b is perturbed, $c(r = 1, \theta, t = 0) = c_0(r = 1, \theta, t_b) - \delta_{per} \cos\theta$, with $|\delta_{per}| < 1$, and used as the initial condition while solving Eq. (1). A spectral element solver, described in detail in [17,22], is used for the numerical solution of (1). The solution methodology for an active disk suspended in a quiescent fluid ($\epsilon = 0$) is slightly different [11]. A value of $R_o = 200$ has been used in all the simulations, after establishing convergence [11]. Using a procedure analogous to that in [23], the stresslet induced by the two-dimensional disk is derived as

$$\boldsymbol{S} = -2\int_0^{2\pi} [\boldsymbol{n}\boldsymbol{v}_s + \boldsymbol{v}_s\boldsymbol{n}]d\theta, \tag{3}$$

where $\boldsymbol{n} = \boldsymbol{e}_r$ is the unit outward normal on the surface of the disk. The expressions for the various components of the 2×2 stresslet tensor have been derived in [11]. Since S_{xx} and S_{yy} are identical in magnitude and differ only by sign, we only present results for S_{xy} and S_{yy} in this paper. In a dilute suspension of noninteracting autophoretic disks, S_{xy} would contribute to the effective shear viscosity of the suspension.

III. RESULTS

Results for an autophoretic disk suspended in a quiescent fluid ($\epsilon = 0$) are presented first (Fig. 1) to provide context for our findings on disks placed in shear flow. The base state for a two-dimensional disk has no fluid flow and time-dependent solute diffusion, which we evaluate by numerically solving the transient diffusion equation. Our approach is in contrast to [12,24] who assume a steady base state, in which the purely diffusive concentration field is set to zero at a finite distance
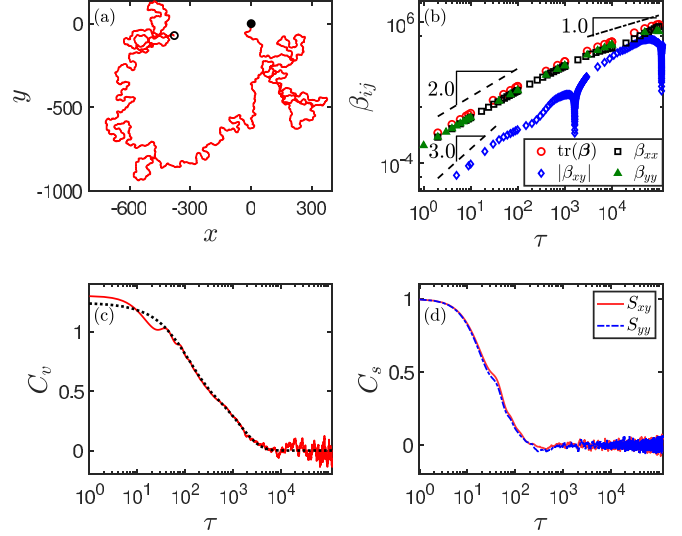

FIG. 1. Dynamics of a two-dimensional autophoretic disk in a quiescent fluid ($\epsilon = 0$) at Pe = 20. (a) Trajectory in the $x - y$ plane; solid and hollow circles denote the beginning and end of the trajectory, respectively, (b) elements of the mean square displacement tensor $\boldsymbol{\beta}(\tau)$, (c) velocity autocorrelation, and (d) stresslet component autocorrelation. The black dotted line in (c) has the functional form $f_1 \exp[-\lambda_1\tau] + f_2 \exp[-\lambda_2\tau]$, with the parameter values given by $f_1 = 0.64$, $\lambda_1 = -0.009$, $f_2 = 0.60$, and $\lambda_2 = -0.0007$.

R_o. In [11] we show that both approaches yield qualitatively similar dynamics in the chaotic regime; however, there are important differences regarding the onset of self-propulsion.

An autophoretic disk in a quiescent fluid undergoes qualitative changes in its trajectory as the Péclet number is increased, evolving from a stationary state to one of steady linear motion, followed by a meandering regime that transitions via an intermittency scenario to chaotic motion at sufficiently large Pe [11,12]. The chaotic dynamics is characterized by a transition to diffusive scaling of the mean square displacement of the particle. We choose a representative value of Pe = 20 that is deep in the chaotic regime. The mean square displacement tensor of the disk at a lag time τ is $\boldsymbol{\beta}(\tau) = \langle [\boldsymbol{r}(t + \tau) - \boldsymbol{r}(t)][\boldsymbol{r}(t + \tau) - \boldsymbol{r}(t)] \rangle$, where $\boldsymbol{r}(t)$ denotes the instantaneous position of the particle at time t and the angular brackets represent the average evaluated over the trajectory of the particle. The off-diagonal components of this 2×2 tensor are identical and the scalar mean square displacement is given by the trace of $\boldsymbol{\beta}$, i.e., MSD $\equiv$ tr($\boldsymbol{\beta}$).

It is seen from Fig. 1(b) that, even though MSD $\sim \tau$ at long times, seemingly indicative of Brownian motion, the displacement cross correlation β_{xy} does not vanish, which is markedly different from a passive Brownian particle. To represent the data on logarithmic axes, we plot the absolute values of the off-diagonal term, β_{xy}. The growth of β_{xy} with respect to the lag time proceeds with abrupt dips, which have been observed by Suga et al. [7] in their experiments on active liquid crystal droplets swimming in a surfactant solution in a two-dimensional geometry. While the overall MSD for the liquid crystal droplets oscillates in time it is the off-diagonal component of the MSD tensor which displays an oscillatory behavior in the present work. Suga et al. [7]

observe that the oscillation in the MSD corresponds to a case where the droplet traces out multiple "figure 8" or looplike patterns. An examination of the disk trajectory in our work [Fig. 1(a)], however, reveals that such looplike patterns constitute only a small fraction of the overall trajectory. There is an early-stage $\sim\tau^3$ scaling observed for β_{xy} whose origins remain unclear. The overall MSD of the autophoretic disk in a quiescent fluid is therefore not oscillatory, but rather exhibits the ballistic-diffusive transition observed previously in numerical investigations [5,12]. The off-diagonal component of the MSD tensor for self-propelled objects has not been examined widely in the literature. Ten Hagen *et al.* [25] consider an active Brownian particle (ABP) model in which the orientation of the particle has a deterministic component stemming from a finite angular velocity, as well as a stochastic component. They present a detailed derivation for the mean square displacement of the particle. Following a similar route, it may be shown that β_{xy} is zero in the absence of an angular velocity, but does not vanish in general for finite values of the angular velocity. This agrees with the intuition that the x and y displacements of a particle moving in two dimensions would be correlated in the presence of a finite, deterministic angular velocity. The velocity and stress autocorrelations are evaluated as $C_v(\tau) = \langle \boldsymbol{U}(t) \cdot \boldsymbol{U}(t+\tau)\rangle / \langle |\boldsymbol{U}(t)|\rangle^2$ and $C_s(\tau) = \langle s(t)s(t+\tau)\rangle / \langle s^2(t)\rangle$, respectively, where s represents either S_{xy} or S_{yy}. We observe that C_v in Fig. 1(c) is well approximated by a sum of two exponentials. The autocorrelation of both the xy and yy components of the stresslet decay nearly identically, going to zero at $\tau \approx 300$ [Fig. 1(d)]. This is to be expected because there is no ambient flow that would lead to a distinction between the components of the stresslet.

A widely used reduced-order framework for self-propelled microscale objects is the ABP [26–28], wherein a particle is assumed to move with a constant speed, while its instantaneous orientation is selected from a Gaussian white noise distribution. Peruani and Morelli [29] (hereafter PM) prescribe a model for a self-propelling particle in two dimensions which allows for fluctuations in both the magnitude and direction of velocity. By assuming that the instantaneous velocity magnitude may be selected stochastically from a Poisson distribution and the orientational distribution function obeys a diffusion equation, they analytically derive an expression for MSD and C_v of such a particle. Both the ABP and PM models predict an MSD that transitions to long-time diffusion following an early-time ballistic behavior. However, while the ABP predicts that a single-exponential may be used to describe the variation in C_v, the PM model posits that the velocity autocorrelation is a sum of two exponentials. In Fig. 1(c), we show agreement with this biexponential form [30] and the computed velocity autocorrelation of an autophoretic disk. It is therefore evident that the velocity time series of an autophoretic disk undergoing chaotic dynamics is better described by the PM model that allows for the instantaneous velocity and orientation to be chosen independently, rather than the ABP model.

For a passive Brownian sphere in shear flow, the mean square displacement in the flow direction (β_{xx}) scales as τ^3 at long times, whereas that in the direction of the shear gradient (β_{yy}) scales linearly with the lag time [31–33]. The cross correlation, β_{xy}, scales as τ^2. The effect of a shear-flow field
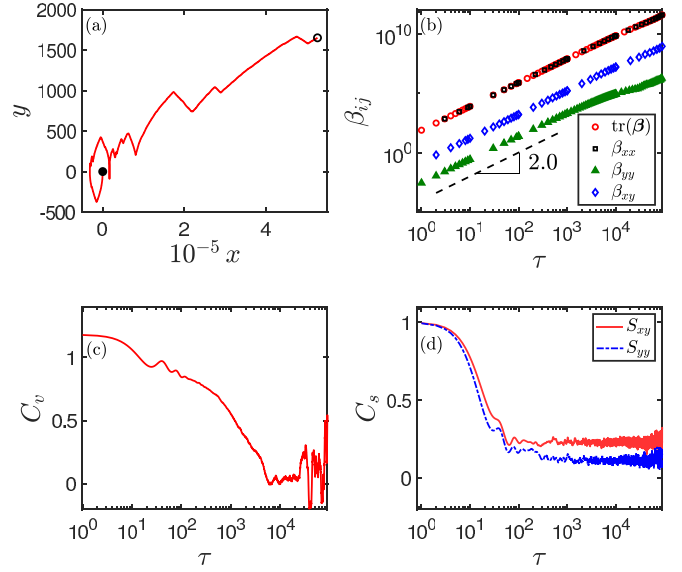

FIG. 2. Dynamics of an autophoretic particle at Pe $= 20$, placed in a shear flow field of strength $\epsilon = 0.01$. The particle is initially at the origin and the flow is in the x direction only, with the velocity increasing linearly with y. (a) Trajectory in the $x - y$ plane; (b) elements of the mean square displacement tensor $\boldsymbol{\beta}(\tau)$, (c) velocity autocorrelation, and (d) stresslet component autocorrelation.

on the dynamics of an autophoretic disk is illustrated in Fig. 2. The position of the autophoretic disk is evaluated as

$$r_y(t + \Delta t) = r_y(t) + U_y(t)\Delta t,$$
$$r_x(t + \Delta t) = r_x(t) + [U_x(t) + \epsilon r_y(t)]\Delta t, \qquad (4)$$

while the expression for the mean square displacement tensor remains unchanged. In Fig. 2(b), the components of $\boldsymbol{\beta}(\tau)$ for an autophoretic disk placed in a shear-flow field of $\epsilon = 0.01$ are plotted as a function of the lag time and it is observed that they all scale as τ^2, in marked contrast to the scaling observed for a passive disk. The autocorrelation of the phoretic velocity is not significantly altered in comparison to the quiescent case [Fig. 2(c)]. The autocorrelation of the stresslet components [Fig. 2(d)] do not vanish in the long-time limit due to the presence of an ambient shear flow. Furthermore, the xy and yy components of the stress tensor may be clearly differentiated from their autocorrelation signals, unlike that in the quiescent case, since the imposed flow has a fixed direction, along the x axis.

A strategy for quenching the chaotic motion of the autophoretic disk is discussed next. In the context of high-Reynolds number applications, the use of magnetic fields [34], buoyant forces [35,36], and mechanical impulses [37] has been suggested to relaminarize the flow [38]. In a similar spirit, recent simulations [17] and experiments [39] have established that an external force field may be used to quench the chaotic variation of the velocity field around an autophoretic particle [40]. In Fig. 3, the effect of increasing the shear strength on the phoretic velocity of the particle at a fixed value of the Péclet number is illustrated, over a representative time window. At low values of ϵ, the time series is chaotic, then gradually settles into a periodic pattern upon increasing ϵ, before vanishing completely as the shear rate is increased
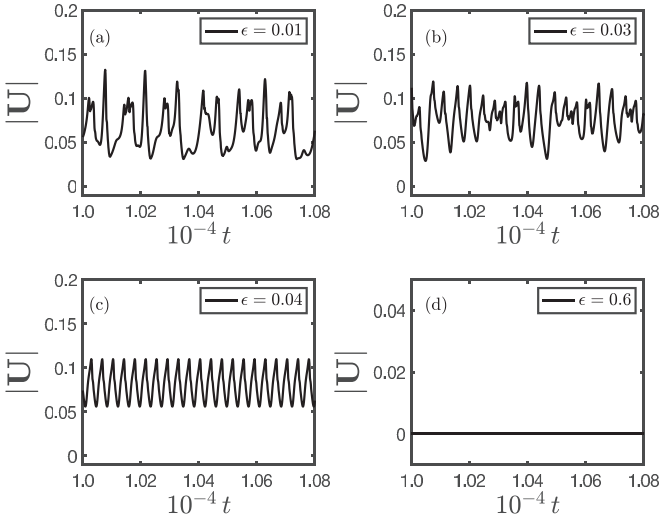
FIG. 3. Time series of velocity magnitude at shear rate values of (a) $\epsilon = 0.01$, (b) $\epsilon = 0.03$, (c) $\epsilon = 0.04$, and (d) $\epsilon = 0.6$, at a fixed value of the Péclet number, Pe = 20.

further. The triangular wave pattern of the phoretic velocity in Fig. 3(c) is qualitatively similar to that predicted for self-propelled two-dimensional droplets [24]. The external flow field, therefore, modulates the self-propulsive motion of the autophoretic disk. A similar trend is observed in Fig. 4 for the stresslet component S_{xy}, which notably attains a time-independent value at sufficiently large shear rates. A negative value for the steady-state stresslet has also been observed for the case of axisymmetric swimmers with a "pusher" type flow pattern [16,23]. We therefore anticipate that a dilute suspension of active droplets would exhibit a chaotic rheology at small values of the shear rate, before first transitioning to a time periodic and ultimately steady rheology as the shear rate is increased.
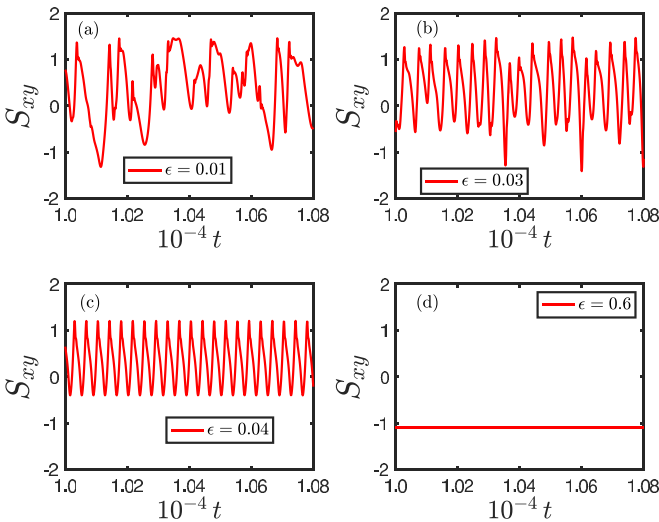

FIG. 4. Time series of xy component of the stresslet at shear rate values of (a) $\epsilon = 0.01$, (b) $\epsilon = 0.03$, (c) $\epsilon = 0.04$, and (d) $\epsilon = 0.6$, at a fixed value of the Péclet number, Pe = 20.
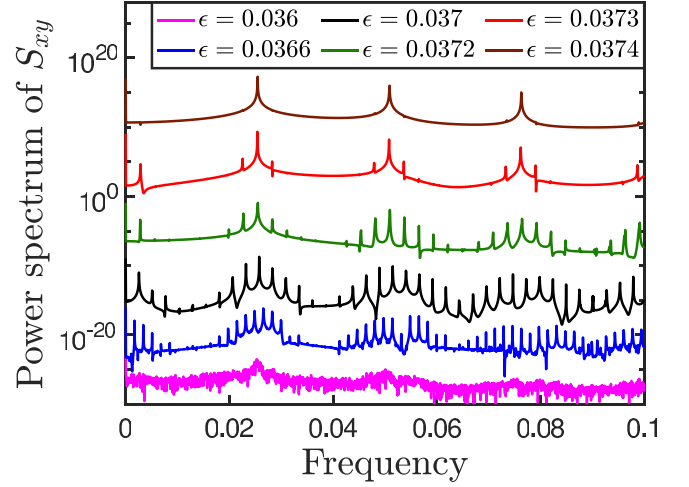

FIG. 5. Power spectrum of the xy component of the stresslet at various values of the shear rate (ϵ) and a fixed Péclet number of Pe = 20. The ordinates of the data series have been multiplied by a scale factor to render them well spaced on the y axis, for clarity. From bottom to top, the values of ϵ (and the associated scale factors) are $0.036(10^{-22})$, $0.0366(10^{-15})$, $0.037(10^{-8})$, $0.0372(1)$, $0.0373(10^{10})$, and $0.0374(10^{18})$.

A more detailed picture of the chaotic-to-steady quenching transition is apparent from the power spectrum of the stresslet, as plotted in Fig. 5 over a narrow window in the shear rate. At $\epsilon = 0.036$, the broadband spectrum signifies chaotic dynamics [41–43]. An increase in the shear rate is accompanied by a coalescence of various frequencies from the broadband spectrum into discrete peaks of the periodic motion in Fig. 4(c). The regularly spaced spikes in the power spectrum at higher values of the dimensionless shear rate, however, do not coincide with integral multiples of ϵ [11].

IV. CONCLUSIONS

We have shown that the dynamics of an autophoretic disk is markedly different from a passive Brownian particle. The dynamics is also richer than that of an ABP with respect to the biexponential decay of the velocity autocorrelation function. Furthermore, we showed that the rheology of a dilute suspension of such disks is chaotic at small values of the shear rate; effectively, increasing the shear provides a route to removing chaotic dynamics. We expect these findings to hold, at least qualitatively, in experimentally realizable dilute active droplet systems, up to an area fraction of $\phi \lesssim 10\%$ based on prior studies on hard-sphere colloidal dispersions [44]. Finally, our work may be useful for the synthesis and manipulation of active droplet emulsions. Here, one may have to account for the coupled chaotic dynamics of many active droplets, which is an interesting direction for future work.

ACKNOWLEDGMENT

[1] Z. Izri, M. N. van der Linden, S. Michelin, and O. Dauchot, Self-Propulsion of Pure Water Droplets by Spontaneous Marangoni-Stress-Driven Motion, Phys. Rev. Lett. **113**, 248302 (2014).

[2] C. C. Maass, C. Krüger, S. Herminghaus, and C. Bahr, Swimming droplets, Annu. Rev. Condens. Matter Phys. **7**, 171 (2016).

[3] S. Suda, T. Suda, T. Ohmura, and M. Ichikawa, Straight-to-Curvilinear Motion Transition of a Swimming Droplet Caused by the Susceptibility to Fluctuations, Phys. Rev. Lett. **127**, 088005 (2021).

[4] J. Decayeux, V. Dahirel, M. Jardat, and P. Illien, Spontaneous propulsion of an isotropic colloid in a phase-separating environment, Phys. Rev. E **104**, 034602 (2021).

[5] W.-F. Hu, T.-S. Lin, S. Rafai, and C. Misbah, Spontaneous locomotion of phoretic particles in three dimensions, Phys. Rev. Fluids **7**, 034003 (2022).

[6] S. Michelin, Self-propulsion of chemically-active droplets, Annu. Rev. Fluid Mech. **55**, 77 (2023).

[7] M. Suga, S. Suda, M. Ichikawa, and Y. Kimura, Self-propelled motion switching in nematic liquid crystal droplets in aqueous surfactant solutions, Phys. Rev. E **97**, 062703 (2018).

[8] B. V. Hokmabad, R. Dey, M. Jalaal, D. Mohanty, M. Almukambetova, K. A. Baldwin, D. Lohse, and C. C. Maass, Emergence of Bimodal Motility in Active Droplets, Phys. Rev. X **11**, 011043 (2021).

[9] D. Müller, A. Otto, and G. Radons, Laminar Chaos, Phys. Rev. Lett. **120**, 084102 (2018).

[10] D. Müller-Bender, R. N. Valani, and G. Radons, Pseudolaminar chaos from on-off intermittency, Phys. Rev. E **107**, 014208 (2023).

[11] See Supplemental Material at http://link.aps.org/supplemental/10.1103/PhysRevE.107.044609 for a justification of the autophoretic disk as a minimal model for active droplet, a discussion of the solution methodology adopted for autophoretic disks in a quiescent fluid ($\epsilon = 0$), convergence studies with respect to the size of the computational domain and the time step width used for numerical integration, expressions for the components of the stresslet $\mathbf{S}$, and a plot of the power spectrum of S_{xy} in logarithmic axes, which includes Refs. [45–47].

[12] W. F. Hu, T. S. Lin, S. Rafai, and C. Misbah, Chaotic Swimming of Phoretic Particles, Phys. Rev. Lett. **123**, 238004 (2019).

[13] J. Anderson, Colloid transport by interfacial forces, Annu. Rev. Fluid Mech. **21**, 61 (1989).

[14] S. Michelin and E. Lauga, Phoretic self-propulsion at finite Péclet numbers, J. Fluid Mech. **747**, 572 (2014).

[15] R. Golestanian, T. B. Liverpool, and A. Ajdari, Designing phoretic micro- and nano-swimmers, New J. Phys. **9**, 126 (2007).

[16] S. Michelin, E. Lauga, and D. Bartolo, Spontaneous autophoretic motion of isotropic particles, Phys. Fluids **25**, 061701 (2013).

[17] R. Kailasham and A. S. Khair, Dynamics of forced and unforced autophoretic particles, J. Fluid Mech. **948**, A41 (2022).

[18] S. Saha, E. Yariv, and O. Schnitzer, Isotropically active colloids under uniform force fields: From forced to spontaneous motion, J. Fluid Mech. **916**, A47 (2021).

[19] Y. Chen, K. L. Chong, L. Liu, R. Verzicco, and D. Lohse, Instabilities driven by diffusiophoretic flow on catalytic surfaces, J. Fluid Mech. **919**, A10 (2021).

[20] H. A. Stone and A. D. T. Samuel, Propulsion of Microorganisms by Surface Distortions, Phys. Rev. Lett. **77**, 4102 (1996).

[21] T. M. Squires and M. Z. Bazant, Breaking symmetries in induced-charge electro-osmosis and electrophoresis, J. Fluid Mech. **560**, 65 (2006).

[22] N. G. Chisholm, D. Legendre, E. Lauga, and A. S. Khair, A squirmer across reynolds numbers, J. Fluid Mech. **796**, 233 (2016).

[23] E. Lauga and S. Michelin, Stresslets Induced by Active Swimmers, Phys. Rev. Lett. **117**, 148001 (2016).

[24] G. Li, Swimming dynamics of a self-propelled droplet, J. Fluid Mech. **934**, A20 (2022).

[25] B. Ten Hagen, S. Van Teeffelen, and H. Löwen, Brownian motion of a self-propelled particle, J. Phys.: Condens. Matter **23**, 194119 (2011).

[26] C. Bechinger, R. Di Leonardo, H. Löwen, C. Reichhardt, G. Volpe, and G. Volpe, Active particles in complex and crowded environments, Rev. Mod. Phys. **88**, 045006 (2016).

[27] M. C. Marchetti, Y. Fily, S. Henkes, A. Patch, and D. Yllanes, Minimal model of active colloids highlights the role of mechanical interactions in controlling the emergent behavior of active matter, Curr. Opin. Colloid Interface Sci. **21**, 34 (2016).

[28] M. Zeitz, K. Wolff, and H. Stark, Active Brownian particles moving in a random Lorentz gas, Eur. Phys. J. E **40**, 23 (2017).

[29] F. Peruani and L. G. Morelli, Self-Propelled Particles with Fluctuating Speed and Direction of Motion in Two Dimensions, Phys. Rev. Lett. **99**, 010602 (2007).

[30] W. Peng, A. Chandra, P. Keblinski, and J. L. Moran, Thermal transport dynamics in active heat transfer fluids (AHTF), J. Appl. Phys. **129**, 174702 (2021).

[31] M. Sandoval, N. K. Marath, G. Subramanian, and E. Lauga, Stochastic dynamics of active swimmers in linear flows, J. Fluid Mech. **742**, 50 (2014).

[32] R. T. Foister and T. G. M. Van De Ven, Diffusion of Brownian particles in shear flows, J. Fluid Mech. **96**, 105 (1980).

[33] P. B. Rhines and W. Young, How rapidly is a passive scalar mixed within closed streamlines?, J. Fluid Mech. **133**, 133 (1983).

[34] H. K. Moffatt, On the suppression of turbulence by a uniform magnetic field, J. Fluid Mech. **28**, 571 (1967).

[35] S. He, K. He, and M. Seddighi, Laminarisation of flow at low Reynolds number due to streamwise body force, J. Fluid Mech. **809**, 31 (2016).

[36] E. Marensi, S. He, and A. P. Willis, Suppression of turbulence and travelling waves in a vertical heated pipe, J. Fluid Mech. **919**, A17 (2021).

[37] J. Kühnen, B. Song, D. Scarselli, N. B. Budanur, M. Riedl, A. P. Willis, M. Avila, and B. Hof, Destabilizing turbulence in pipe flow, Nat. Phys. **14**, 386 (2018).

[38] T. J. Hanratty and Y. Mito, A unifying explanation for the damping of turbulence by additives or external forces, Flow, Turbul. Combust. **83**, 293 (2009).

[39] A. C. Castonguay, R. Kailasham, C. M. Wentworth, C. H. Meredith, A. S. Khair, and L. D. Zarzar, Gravitational settling of active droplets, Phys. Rev. E **107**, 024608 (2023).

[40] H. Stark, Swimming in external fields, Eur. Phys. J. Spec. Top. **225**, 2369 (2016).

[41] K. Ikeda, H. Daido, and O. Akimoto, Optical Turbulence: Chaotic Behavior of Transmitted Light from a Ring Cavity, Phys. Rev. Lett. **45**, 709 (1980).

[42] Y.-C. Lai, Analytic signals and the transition to chaos in deterministic flows, Phys. Rev. E **58**, R6911(R) (1998).

[43] R. C. Hilborn, *Chaos and Nonlinear Dynamics*, 2nd ed. (Oxford University Press, New York, 2000).

[44] D. R. Foss and J. F. Brady, Brownian dynamics simulation of hard-sphere colloidal dispersions, J. Rheol. **44**, 629 (2000).

[45] M. Morozov and S. Michelin, Nonlinear dynamics of a chemically-active drop: From steady to chaotic self-propulsion, J. Chem. Phys. **150**, 044110 (2019).

[46] J. R. Blake, Self propulsion due to oscillations on the surface of a cylinder at low Reynolds number, Bull. Aust. Math. Soc. **5**, 255 (1971).

[47] D. Sondak, C. Hawley, S. Heng, R. Vinsonhaler, E. Lauga, and J. L. Thiffeault, Can phoretic particles swim in two dimensions? Phys. Rev. E **94**, 062606 (2016).